Research paper ■

Sodium Weighted Clinical Brain Magnetic Resonance Imaging at 4.23 Tesla and Inversion Recovery Pulse Sequence

Rakesh Sharma

Abstract. Application of advanced 4.23 T MRI clinical imager was demonstrated for sodium magnetic resonance (MR) data acquisition. Primary hypothesis: Sodium [Na] in brain is MR visible. Secondary hypothesis was, if, application of multislice spin echo (MSSE) pulse sequence at selected scan parameters can sufficiently visualize the total sodium signal as indicator of sub-clinical activity. A new inversion recovery pulse sequence is proposed for selectively suppressing extracellular sodium to visualize extracellular sodium images. Methods: MSSE pulse sequence technique was used to simulate sodium images of human brain. Phantom of sodium and rat brain were imaged and validated. Results: MSSE pulse technique enabled to visualize the sodium signal at selected scan parameters. Specifically, MSSE pulse technique enabled the identification of different sodium rich areas in the brain, comparable with proton MRI images. Reconstruction images of brain further enhanced the power to classify the brain tissue. Intracellular sodium image of tube phantom were generated by use of inversion recovery pulse sequence. Conclusion: Using MSSE pulse sequence at 4.23 T, in vivo sodium images can be generated in times acceptable for routine clinical brain examination with better sub-physiological information as obtained from proton MRI.

The paper was presentation as finalist Computer Based Medical Systems 2002 award manuscript.

■ **Infor Med Slov**: 2005; 10(1): 56-72

Author's institution: Departments of Radiology and Medicine, Columbia University, New York, NY 10032.

Contact person: Rakesh Sharma, Departments of Biological Psychiatry, Columbia University, New York, NY 10032.
email: rs2010@Columbia.edu.

Introduction

Integrated approach of Proton MRI with in vivo sodium magnetic resonance imaging seems promising to detect sub-physiological abnormalities. Sodium nuclei inside the brain exist in free and bound forms as extracellular and intracellular sodium populations exhibiting longer and shorter relaxation times respectively reported.[1] Sodium moves in free form or also bound with proteins, glycosides via a site localized on the exterior surface of cell membranes. Most of the Na nuclei undergo substantial relaxation before their signals can be acquired. Sodium has a spin of 3/2 and a quadruple moment. So, sodium exhibits many energy transitions and two transverse relaxation times, a long T2 = 16-30 ms and a short T2 = 0.7-3.0 ms depending upon magnetic field strength.[2] To acquire sodium images in experimental animals and human, multiple quantum (MQF), single quantum (SQF), triple quantum (TQF) filter methods have been used highlighting the need of high magnetic field at 4.23 Tesla imager as reported.[3-7] Several 2D and 3D spin echo and gradient echo pulse sequences have been in use. Until this date, sodium brain images in clinical set up at higher magnetic fields such as 4.23 T have not been reported perhaps due to two reasons: less sodium abundance and less sensitive intracellular sodium nuclei in the body. Present study reports here initial attempt to capture the intracellular sodium images using inversion recovery pulse sequence and demonstration of sodium MR images comparable with proton MR images in order to establish the utility of proton-sodium images by use of double tuned probes. Although, sodium distribution is not identical to the proton distribution in the brain it can vary independently in a multitude of physiological and pathological conditions. For interested readers, comparison of different pulse sequence methods is demonstrated and the source code of sodium imaging inversion recovery is included as Appendix 1 at the end.

Theory of Sodium Imaging and contrast in brain: In the brain, 23Na concentration is 0.14 to 0.16 M in the extracellular space while 0.012 to 0.02 M in the intracellular space about 8-20% of total brain volume. This extracellular space is significant in sodium MR imaging as sodium increases sharply in the diseases like edema. The average concentration of sodium in a volume of brain tissue that comprises both intra- and extracellular compartments is approximately 0.045 M. Integrated approach of proton and sodium MR imaging is significant in evaluating sensitivity and contrast to different brain regions. The contrast solely depends on spin density and relative concentration of sodium and protons in the brain ventricles (filled with cerebrospinal fluid CSF) in the following manner: $C = (I - I')/ I'$, where I is the signal intensity received from the region of interest and I' is the signal intensity received from the background. In the case of brain, region of interest happens ventricles while the background is surrounding brain tissue. Based upon the literature, the concentrations of proton and sodium nuclei show that brain / ventricle contrast is 7.9 times greater on sodium images than on proton images as reported.[8] Despite of it, sodium image contrast in normal brain cells suffers from "poorly MRI visible" intracellular sodium due to its shorter T2. In the cerebrospinal fluid (CSF) and extracellular space, the sodium is adequately "MRI visible" due to much shorter T2 shown.[9] The contrast in proton imaging depends upon the relaxation times as T1 and T2-contrast although these relaxation time constants do not correlate with proton concentration. We developed a approach to selectively suppress extracellular sodium using inversion recovery pulse sequence based on using optimized inversion times to generate sodium MRI contrast power to define possibly brain regional physiology and tumor physiology in animal tumor models reported.[10]

In terms of sodium MR measurements we need average sodium image intensity from both the single quantum and inversion recovery images, as well as single quantum image values for the sodium phantom. For the composition of intracellular sodium inversion time (T_i), we need the inversion time, which produces the lowest values for the brain tumor image intensity. The

equation for S, relating signal attenuation as a result of an inverting pulse can be given by

$$S = N[1 - 2\exp(-TI/T_i) + 2\exp(-(TR - TE/2)/Tl) - \exp(-TR/T1)]\exp(-TE/T2) \quad \text{Eq.1}$$

where N. f[T1,T2,TR,TI] is the attenuation function, which for short TE and long TR and T2, can be approximated as N. f (T1, TI). These functions give the relative dependence on the various time constants and pulse sequence intervals. The constant "N" is a function of units, equipment amplification, field strength and others instrumental parameters. Using the selected phantom just described with equation above, "N" can be determined. This equation can be used to estimate single quantum images without inversion pulses by setting the inversion time = 0. The multislice spin-echo Na MRI pulse sequence was used with repetition times on the order of 100 msecs and spatial resolutions on the order of 1 mm. During the course of a pulse cycle sodium nuclei are moved by diffusion between microscopic domains, or interchange bound to unbound. It smears the distribution of real T1 values while giving a stable composite T1, which appears well behaved in response to the inversion pulse.

Methods and Materials

MR data acquisition: In our imaging experiments a multislice spin echo (MSSE) pulse sequence was used at Hatch NMR Center, Columbia University, New York, NY as described elsewhere.[1] The short echo was obtained at TE=5.6 ms. The signal from short T2 fraction of intracellular sodium was not detected and only 40% of the sodium signal arising from brain was detected due to very low "MRI visible" sodium abundance around 1/5000 than the abundance of protons. The clinical sodium images were obtained on 4.23 Tesla whole body MRI system operating at a Larmor frequency of 52 MHz (see Figure 1). Thus NMR sensitivity of sodium was 9.25% that of protons at the same magnetic field at 4.23 T. Sodium NMR signals from single echo for a given volume of brain was only 1/54000 of the signal obtained from the protons at the same field. This weak sodium signal was attenuated by the following approach using: short TR =100 ms; higher relaxation of spatial resolution 4 mm; observation time = 6 ms.

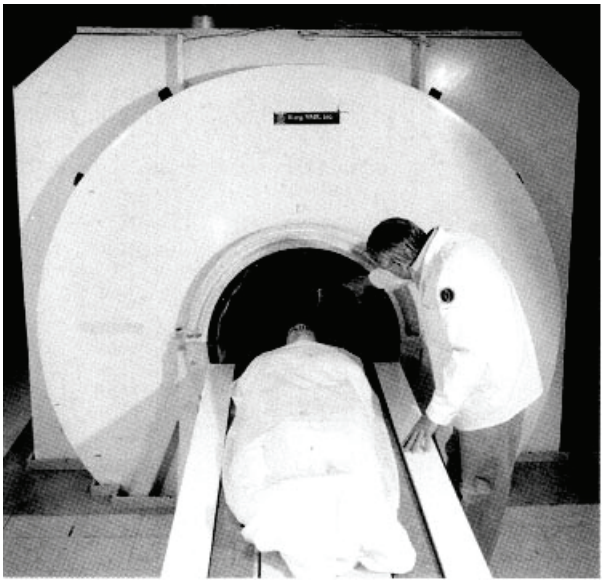

Figure 1 A human 4.23 Tesla Magnetic Resonance Imaging clinical imager with wide bore of 67 cm equipped with state of art superconducting magnet.

3-D gradient echo data acquisition techniques (see Figure 2) were used for the observation of sodium at every point of the brain. For it, 3D slab gradient echo pulse was used employing inversion pulse in acquisition data matrix 64 x 64 x 24 covering the entire volume of human head to acquire 24 slices, each 1 mm thick, in 34 minutes providing additional signal averaging. In sodium brain images, gray / white matter discrimination was seen on scans showed in-plane resolution of 4 mm. Proton images were acquired by 3-D multi-spin short echo spectroscopic imaging pulse sequence at spin echo times TE= 10 and 12 ms, TR=100 ms, FOV= 90 cm, 128 x 128 matrix with total spectroscopic imaging time 46 minutes. Regional sodium concentration was estimated by a local fitting program, estimating M_o= 145 mM (in vitreous humor of eye) and relative sodium values in other regions.

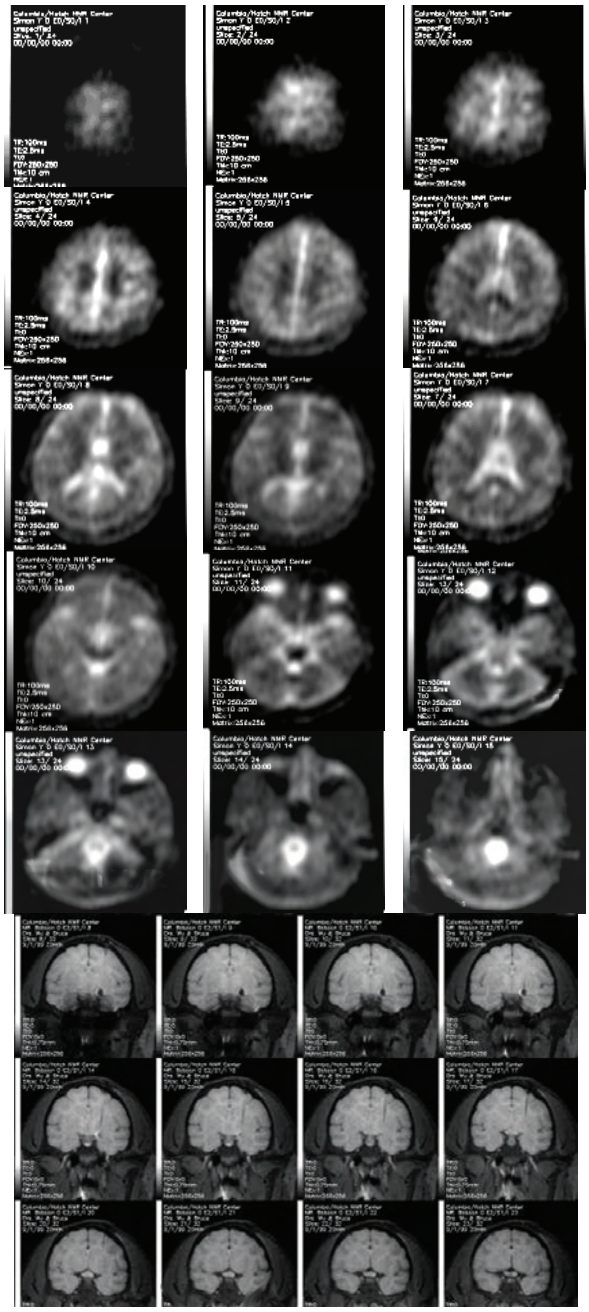

Figure 2 Axial T1 weighted 23Na sodium MR human normal brain images acquired at 4.23 Tesla MRI clinical imager. Images were acquired at TR=100 ms, TE = 5.6 ms, TI= 25 ms, slice thickness = 2.5 mm, matrix 64 x 64 x 34, data points 1048. Axial brain images are shown top left towards down right for superior towards inferior slices. Coronal brain images are shown at bottom from frontal to parietal slices. At same level proton MRI images are shown in Figure 7 with approximate levels of 3 slices in reconstructed images in Figure 7 lower panels, middle row.

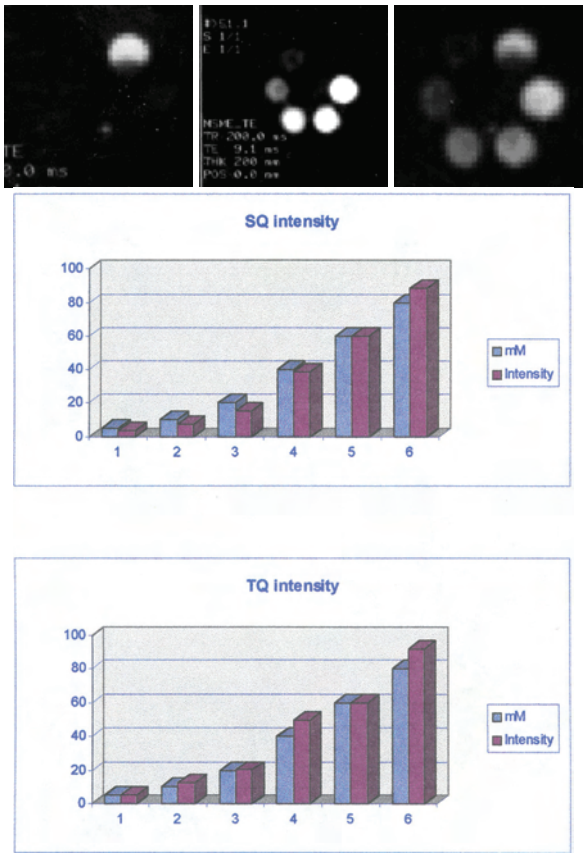

Figure 3 Phantom for comparison of SQ and TQ methods and validation was performed in 7 tubes filled (middle and right panels on top) with different concentrations of NaCl as shown in graph with their image signal intensities (Panels on bottom). For comparison, inversion recovery method was used for these phantom tubes that showed insensitive IR sodium signal to these tubes but high signal for lowest NaCl concentration (left panel on top). The signal intensities and concentrations change proportionately in both SQ and TQ methods.

Sodium concentration and MR image intensity experiments: 7 tubes filled with different increasing NaCl concentrations were arranged in a circle (see Figure 3) for projection (transaxial) imaging at TR=130 ms and resolution 100/64 mm. For Comparison and validation purposes, standard single quantum (SQ) by spin-echo at TE=9 ms, number of averages=96, imaging time=96 x 64 x 0.13 or 13 minutes 20 seconds. For better imaging Triple quantum (TQ) images acquired by using 12 steps of refocused RF pulse in the evolution period were obtained in creation

time =14 msec, number of averages = 1920 within four and half hours.

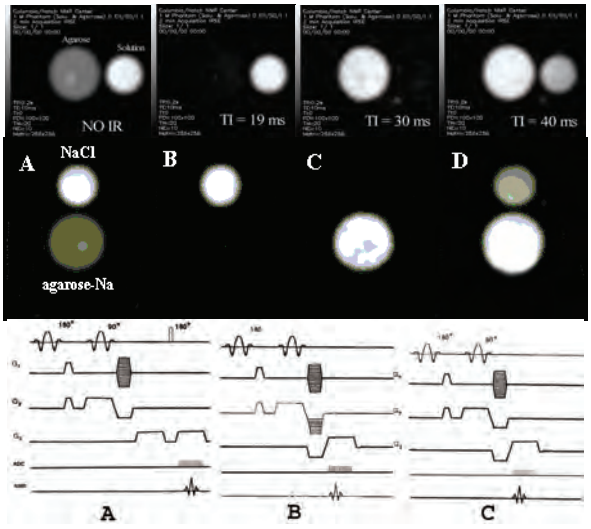

Figure 4 For experiments on intracellular sodium (on bottom), 2D spin echo sequence is shown as sequence diagram (A) to differentiate intracellular and extracellular sodium in a phantom model system. The phantom consists of two tubes, one is 1 M NaCl in solution and the other is 1 M NaCl in 4% agarose (Panel A). They simulate extracellular and intracellular sodium, respectively without use of inversion recovery pulse. It can be seen that an inversion time of TI=20 ms completely suppressed intracellular sodium (Panel B) and TI=30 ms completely suppressed the extracellular sodium signal from the tube containing NaCl in solution (Panel C). At TI=40 ms partial suppression of extracellular sodium is highlighted (Panel D). Acquisition parameters were TR=200 msec, TE=3.2 msec, matrix 258 x 258. For extracellular sodium and intracellular sodium images, conventional 2D-slice selective gradient echo is shown as diagram (B) and 3D-slice selective gradient echo sequence diagram (C).

Intracellular sodium MR phantom and validation: 2-D spin echo sequence was used to differentiate intracellular and extracellular sodium in a model system (see Figure 4). The phantom was made of two tubes, one had 1 M NaCl (representing extracellular sodium) in solution and the other had 1 M NaCl in 4% agarose to simulate increased viscosity and binding sites of intracellular space (representing intracellular sodium) as shown in Figure 3. These tubes simulate extracellular and intracellular sodium images, respectively without use of inversion recovery pulse.

The extracellular sodium and intracellular sodium images were acquired with a conventional 2D-spin-echo inversion-recovery pulse sequence (IR). To validate the power of IR pulse sequence and variable inversion times (TI) to distinguish sodium populations, different TI= 10, 20, 30 ms were used. Acquisition parameters were TR=200 msec, TE=3.2 msec, matrix 258 x 258. IR pulse sequence was used to suppress contribution of sodium within a specific range centered around T_1^{ex}. Having identified this range, inversion time was set to TI=(ln 2)(T_1^{ex}), at long repetition times (TR). In these experiments, by hit and trial error, we set optimal TI=25 ms to suppress composite signal mainly from extracellular sodium. For demonstrating two different null points of intracellular and extracellular sodium populations, different "tau" values represented exponential sodium MR signals rising at different rates. It highlights the existance of two populations of sodium in MR signal with predominent extracellular sodium. Phantom studies in our system were designed for a contrast sensitivity of 0.05 mM of sodium in a disc 10 mm in diameter, for a 1-cm thick slice.

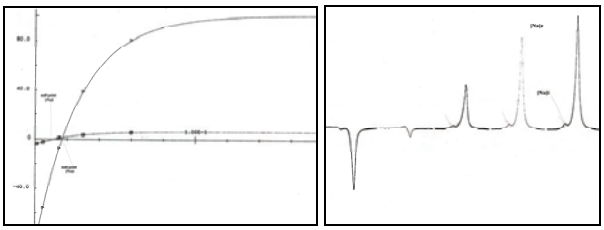

Figure 5 Na-23 MR spectrum is shown to demonstrate different null points crossing on x axis at two different "tau" values representing higher signal for extracellular sodium and lower signal for intracellular sodium. Exponential sodium signal (ln 2)(T1ex) is represented as rising IR amplitude (left figure) and their respective two different chemical shift peaks rising at different time intervals (right figure). However, intracellular sodium peak appears very small in absence of shift reagent, shown with small arrows in the right panel. In presence of shift reagent it becomes prominently larger.

Rat brain imaging: For quality control purposes, rats were placed on horizontal plateform and small Rf coil was chosen with following dimensions: inner diameter 44 mm,outer diameter 50 mm single turn, saddle (non-quadrature type), with SNR 2.4 times better than large coil. Transaxial and coronal projection images were obtained at TR=130 msec, number of averages = 120 in 17 minutes (for SQ) and 960 minutes (for TQ) (see Figure 6).

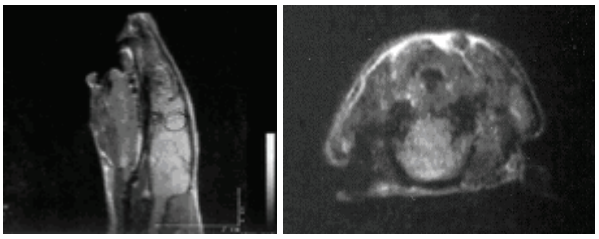

Figure 6 Rat images are shown as transaxial (left) and coronal projections (right) at TR=130 ms, Number of average=120 (SQ) and 960 (TQ).

Results

Sodium weighted data acquisition time and sensitivity of the method: A series of sodium axial and coronal T1 weighted images of the head of a normal volunteer is illustrated in Figure 5. It was difficult to discriminate CSF in the subarachnoid space from cortex in Na MR images. CSF and fluid-filled regions like ventricles and eyes showed slow T2 decay while cortex showed fast T2 measurements. The images are sequential cross-sectional representation extending from top of the head in the upper left panel to lower right panel at the level of eyes. In the first row, images showed sodium distribution almost uniform in upper parietal region. In the second row, images show the bright signal arising from CSF surrounding the brain in the subarachnoid spaces. The brain parenchyma appears darker than the surrounding CSF. The two lateral ventricles and the Sylvian fissure can be seen brighter in third and fourth row images. The suprasellar and perimesencephalic cisterns can be seen on the right images in fourth row and bottom left image. The eyes show strong signal because of the large extracellular compartment in both vitreous and aqueous chambers. In the bottom right images, medulla oblongata rich in CSF can be seen in coronal images.

We compared different concentrations of sodium NaCl (as free extracellular sodium) for their sensitivity on SQ and TQ images. Sodium concentration and image signal intensity on SQ images showed better linear relationship over the TQ images (see Figure 3). However TQ images exhibited more sensitive for intracellular sodium (bound sodium) with short T1. The TQ image acquisition time was considerably long than the acquisition time for SQ images. So, we preferred inversion recovery method to suppress extracellular sodium signal.

Table 1 Axial human brain proton MRI and 23Na MRI imag slices were co-registered and compared by delineation of area of brain by Optimas 6.5. The area was matched and statistically analyzed in different slices (n=14).

Brain Slices (n=14)	Area measured on Proton MRI (in mm^2)*	Area measured on 23NaMRI (in mm^2)**
1	0.5048	0.4702
2	0.4666	0.4404
3	0.4001	0.3528
4	0.5132	0.4559
5	0.7708	0.7729
6	0.6779	0.6641
7	0.9372	1.0358
8	0.9716	0.9456
9	0.3764	0.3732
10	0.6180	0.5924
11	0.5480	0.5216
12	0.3001	0.2959
13	0.5928	0.5683
14	0.5404	0.5539

Statistical analysis: Slope 0.9890±0.0168; 95% Confidence Intervals 0.9528 to 1.025; P value<0.0001

Comparison of proton weighted T1 and sodium weighted data acquisition time and sensitivity of the method: The reconstructed images are shown in Figure 7 for brain landmarks. Co-registration of proton and sodium image showed good

comparison as illustrated (bottom row images) for total brain cross-sectional area (r^2=0.9830; p=0.0001) for (n=14) measurements in Table 1.

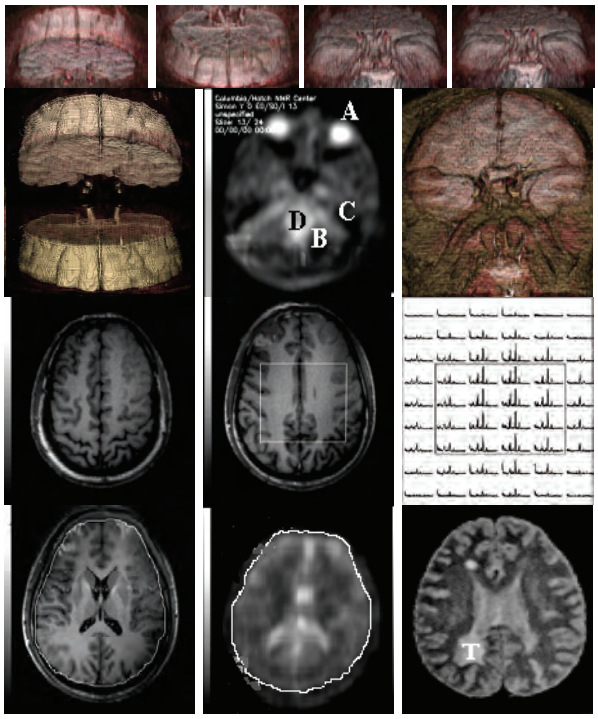

Figure 7 Contiguous brain slices are shown as axial re-construction images by rendering method (top row), parietal lobe structures in the brain in the second row (axial image, left panel) and coronal image, right panel) with matched sodium image (middle panel) represent good comparison and sodium distribution (A for eye 145 mM; B for ventricle 85 mM and C for cortex/subarachnoid space 25 mM; D for CSF 142 mM). In third row, contiguous proton axial T1 images and localized brain spectra (rightmost) are shown. As illustration for the comparison, proton T2 axial image (on left, bottom), intracellular sodium T1 axial image (on middle, bottom) and brain tumor image (on right, bottom) with tumor (T) are shown with brain area delineation by Optimas 6.5 program. For sodium, multislice spin echo IR pulse sequence, scan parameters were:TR=100 msec; TE=5.6 msec; FOV=40 mm, slice thickness=2.5 mm; flip angle=90°; TI=25 msec; acquisition matrix=64x64x34. For proton, multislice short echo IR pulse sequence was used with:TR= 200 msec;TE= 10 and 12 msec; slice thickness=2.5 mm; matrix=128 x 128.

These measurements were comparable showing difference less than ±5% by using both methods (Figures 7 and 8). However, the comparison may suffer from the software characteristics to delineate the brain area and measure area. For demonstration, a representative brain tumor is highlighted marked as "T" which clearly signifies the value of high sodium MR signal inytensity of tumor. In the clinical observations the signal intensity determined from the NMR images of the normal volunteers show that the lateral ventricles provide a sodium signal four times larger than that obtained from the surrounding brain parenchyma.

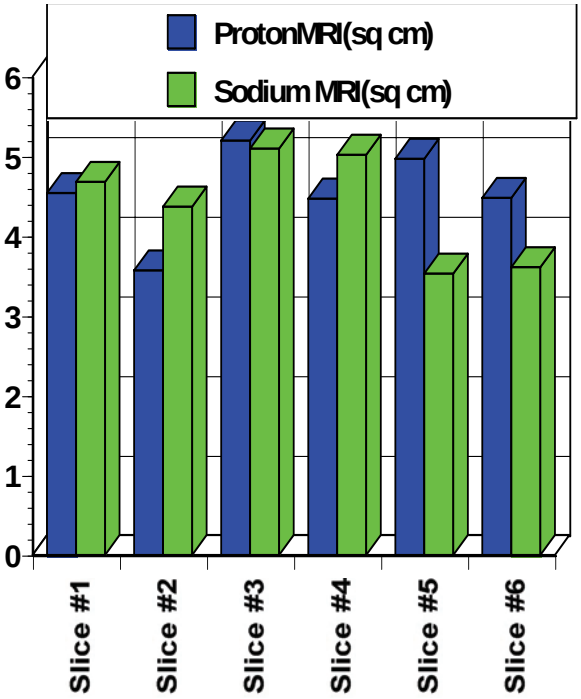

Figure 8 Measurements of brain delineated area for six different levels are shown by proton MRI method and sodium MRI method. One representative slice image by proton MRI and sodium MRI image with delineation lines by Optimas software at same level are shown in Figure 2. Both methods showed approximately same measurements and comparison (top panel) showed insignificant statistical difference at 95% confidence limits for the data shown in Table 1.

Multislice spin echo method was specific to sodium nuclei. The sodium concentration in the different brain locations may be derived from literature on compartmental size varying 25 mM in white matter and 47 mM in cerebral cortex, which were comparable with our fitted program based

sodium concentration mean values in white matter, cortex, CSF, superior sagittal sinus. Although several artifacts were obvious for interpreting sodium concentration in brain such as partial volume effects, centrum semiovale region, nonuniform radiofrequency field, CSF or vitreous humor as standard extracellular sodium concentration etc. Moreover, effects of inhomogeneous radiofrequency field were negligible at short echo (early echo) reported[4] due to reported more brain signal at short TE (3.6 ms) than with long TE (14 ms) for MR "visible" fast T2 components of brain sodium. The standard extracellular sodium concentration (145-mM) by extrapolated M_o values may be erroneous because of multi-exponential free induction decay of sodium. However, sodium concentrations in identical regions with similar T2 decay may be good comparison such as cortex and white matter.

Optimization of inversion time in sodium phantom imaging: Using inversion recovery pulse sequence (see Apendix 1), at lower inversion time (TI) range, both free extracellular and bound intracellular sodium showed higher signal intensity decreasing in the inverse manner with rise in TI. Surprisingly, free extracellular sodium exhibited higher sodium signal intensity at the TI = 20 msec (in Figure 4), which remained high till TI < 25 msec. At TI = 30 msec, bound sodium or intracellular $[Na]_i$ exhibited higher signal intensity while free sodium or extracellular sodium was not visible. These altered signal intensities may be seen on phantom images as shown in Figure 3. Sodium MR signal intensity was 4 – 6 times lower than the proton MR signal intensity in the brain as shown in Figure 2 middle panels.

Discussion

Na-23 is second most abundant MR sensitive nucleus next to proton. So, it has its magnetic resonance (MR) imaging potential. The presence of two well-defined sodium intracellular and extracellular compartments in brain provides regional information on relative size of compartments. The first use of higher magnetic field strength at 4.23 Tesla with the use of lower noise electronics with more sensitive radiofrequency (RF) antenna provided the ease of MRI operation and better sodium MR visibility of CSF, venous spaces and cortex. On contrary, white matter is relatively sodium free. Short TR = 100 ms than that used in proton images TR = 0.2 – 2.0 sec, utilizes the advantage of relatively short T1 of sodium. Sodium fast relaxing nuclei exhibit high spatial resolution around 4 mm (for proton it is 1 mm). The observation time 4 to 6 ms for sodium was another advantage for optimal clinical evaluation best achieved by imaging the entire head. In the case of sodium imaging in particular, noise was the limiting factor. Total volume 3-D imaging approach of brain appeared the most desirable, without much to be gained by limiting the number of observed slices. In any 3 D data acquisition scheme, limiting the size of the imaging region-of-interest by reducing the number of observed planes does not result with faster NMR signal acquisition in a given imaging time and resolution. Sodium imaging seems a suitable clinical diagnostic approach using multislice spin echo Na-MRI method due to the major involvement of sodium in important dynamic processes in the cell. Free extracellular sodium concentration $[Na]_e$ depends on the metabolic energy for homeostasis and calcium, hydrogen ions through coupled exchangers in the brain.

From biomedical standpoint of sodium signal source in brain, each cell gets metabolic energy through the biosignal processing so called "trans-membrane active potential" of cell across sodium-potassium ion channels. These channels do function at the expense of metabolic energy ATP controlling the sodium and potassium transport known as "sodium pump" and biochemical phenomenon is known as "Na^+/K^+ ATPase enzyme system". High concentrations of extracellular sodium protect loss of intracellular sodium naturally. However, in abnormal situations in the cell tend to force the ATP metabolic energy to activate ion-channels to allow only limited amounts of intracellular sodium to leave the cell and cross the membrane. This type of activated

process causes "activation potential" generation and drop in cell membrane electrical activity or threshold membrane voltage to maintain to Na^+/K^+ ion balance overall in side the cell. Presumably, this small subphysiological energy exchange during intracellular sodium transport provides the opportunity to generate the magnetic resonance effect as visible spin echoes at different quantum levels such as single-, double-, triple-, multiple quantum filters. Henceforth, this property generates sodium as MR visible by using different pulse sequences based on sodium quantum levels.

We have used in our lab these different pulse sequences such as single-, double-, triple- and multiple quantum filter methods as reported.[2,6-8] Other recent fast 3D sodium brain imaging studies were reported using 2.0 MR clinical imager[11] based on fast T(2)(*) relaxation component between 1.2-1.6 ms and slow component T(2)(*) between 7.1-8.4 ms. Alternative approaches for sodium quantification using regional T2 values and sodium measurements by extrapolated equilibrium magnetization (M_o) and multiple short echo pulses using short T2 (0.7-0.8 ms) and long T2 (7.0-26.0 ms) are still in infancy. However, sodium-imaging studies are limited. Recently double tuned sodium coils were reported for apparent diffusion coefficients (ADC) imaging in focal cerebral ischemia to highlight accumulation of sodium in dead tissue.[12]

To our knowledge, intracellular sodium MR properties seem to be very dependent upon selection of scan parameters such as variable inversion times (TI) and (TE) as shown in Figure 3. Still, there is trade-off between high magnetic field with imaging long acquisition time and achievement of absolute intracellular sodium signal by suppressing majority of extracellular sodium signal. Henceforth, the sole approach of the inversion recovery effect without use of any contrast agent injection appears valuable and needs shorter image acquision time than its counterpart TQ method. This fact of inversion recovery effect on high intracellular sodium rich fluid containing parts of the brain and phantom can be observed (see Figures 3 and 4) where in Figure 3 intracellular phantoms appear brighter and extracellular or free sodium signal appear completely suppressed. This fact further highlights the necessity of inversion recovery effect due to its longer rise time of longitudinal magnetization for T1 and superiority of inversion recovery pulse sequence. Nevertheless, complete suppression of extracellular sodium MR signal is not possible in tissue imaging because of the fast dynamicity of sodium in the brain and cells. This fact is demonstrated in rat images where transaxial images showed poor SNR. Relatively, use of higher magnetic resonance fields may enhance the selective sodium MR visibility in future to answer pathophysiological conditions of brain.

Sodium is altered in many other pathophysiological conditions of clinical interest; and hence, is an indicator for many types of pathology including colon, uterine malignancy, arrhythmia and stroke as reported.[2] Recently, emphasis was shifted to study the cause of increased intracellular sodium in neoplasia vs normal tissue, malignant vs benign tumors and poorly differentiated vs. well-differentiated tumors as reported.[13] Antineoplastics can change cell cycle distribution often leading to apoptosis as a result, both changes in cell cycle phase and apoptosis alter intracellular sodium $[Na]_i$.[14] For this intracellular sodium $[Na]_i$ change, due to its multiple spin state transitions, it needs be examined through specific pulse sequences where selectively molecular target imaging in cancer tumors, may answer enhanced antineoplastic drug cytotoxicity e.g. gene expression imaging. Higher ratios of intracellular Na^+/K^+ in both benign and malignant tumors over their normal cellular counterparts were recently reported.[15] Increased intracellular sodium $[Na]_i$ have been well-described fact in a variety of biological systems during normal and pathophysiological events relevant to chemotherapy including movement throughout the cell cycle, apoptosis, necrosis, metabolic suppression, and transformation from normal to neoplastic tissue. $[Na]_i$ changes occur within minutes or hours in response to transmembrane flux alterations or subcellular sequestration.

Whereas proton MRI, which uses the hydrogen nucleus, is ideal for morphological tumor studies, while Na-MRI seems ideal for sub-physiological imaging due to its major involvement of Na in cellular dynamic processes and sodium interaction with chemotherapy, cellular apoptosis and ions. We attempted proton spectroscopic imaging of brain and we could get in vivo information of different metabolites as shown in Figure 2 (middle panels). High resolution of this metabolite information encouraged us to look over sodium spectroscopic imaging possibility. This possibility now seems very feeble due to very weak sodium signal without use of shift reagent. Alternatively, use of inversion recovery pulse appeared unique power to visualize intracellular sodium. With advanced software and magnetic resonance methods, we presume it would be possible to get sodium spectroscopic images. Other main advantage of this sodium MR imaging method is no use of shift reagents to enhance contrast-noise-ratio (CNR). To establish the sodium MR signal and sodium images of brain, sodium images could be compared with well MR visible proton images. However, the comparison may suffer from the software characteristics to delineate the brain area and measure the brain area. Results show statistical agreement in measurements by both methods.

Superiority of sodium MR imaging method over other *in vivo* methods can be attributed due to its capability of extracting out sodium ion changes in membranes actively participating in drug induced sodium transport alterations, screening the drug induced effect on molecular targeting in cancer tissue cells as reported by Sharma et al., 2001. In near future, several cellular targets may be imaged possibly altered by sodium ion activity such as MR active ligands bound with sodium-linked gene, Na^+/K^+ ATPase, reflecting molecular targets of neoplasia, destruction of actin filaments, microtubules, gene expression and suppression of protein synthesis and metabolism.

Conclusion

Sodium human brain images were acquired by rapid, *in vivo* sodium-23 magnetic resonance imaging using non-invasive *multiple quantum filtered* multislice spin echo pulse method. Intracellular sodium and extracellular sodium phantoms demonstrated the power of *multiple quantum filter* to suppress either extracellular or intracellular sodium population at different inversion times. Sodium images showed comparable contrast with respective proton images with diagnostic accuracy. The method may enable the interpretation of borderline malignancy, histologically difficult tumor composition and drug monitoring in clinical set up. Still it is very early to predict the power of sodium MRI in clinical utility and needs further investigations and validation.

Acknowledgements

Author acknowledges Dr. Ed X.Wu, Ph.D. and Dr.JK Katz at Columbia University, New York and Professor R.K.Gupta at Albert Einstein College of Medicine, New York for their laboratory facilities.

Literature

1. Hilal, SK, Moudsley AA, Ra JB et al. In vivo NMR imaging of sodium-23 in the human head. *J. Computer Assisted Tomography* 1985, vol 9, 1-7.
2. Dizon, J M, Tauskela JS, Wise D, Burkoff D, Cannon PJ, Katz. Evaluation of Triple-quantum-filtered 23Na NMR in monitoring of intracellular Na content in the perfused heart: Comparison of intra- and extracellular transverse relaxation and spectral amplitudes. *Magn. Reson. Med.* 1996, Vol 35, 336-345.
3. Permann WH, Turski P, Houston L.,Glover GH, Hayes CE Methodology of in vivo human sodium NMR imaging at 1.5 Tesla. *Radiology* 1986, vol 160, 811-820.
4. Ra JB, Hilal SK, Cho ZH A method for in vivo MR imaging of the short T2 component of sodium-23 *Magn Reson Med.* 1986, vol 3, 296-302.
5. Ra JB, Hilal SK, Oh CH An algorithm for MR imaging of the short T2 fraction of sodium using the FID signal *J.Comput Assist Tomogr* 1989, vol 13, 302-309.

6. Jung K J, Katz, J. Chemical-shift-selective acquisition of multiple –quantum filtered 23-Na signal *J Magn. Reson.* 1996 vol 112, 214-227.
7. Jung KJ, Katz J, Boxt LM, Hilal SK, Cho ZH. Breakthrough of single-quantum coherence and its elimination in double-quantum filtering. *J.Magn.Reson.* 1995, vol 107, 235-241.
8. Hancu I, Boada FE, Shen GX Three-dimensional triple quantum-filtered 23-Na imaging of in vivo human brain. *Magn.Reson.Med.* 1999, vol 42, 1146-1154.
9. Winkler SS, Thomasson DM, Sherwood K., Permann W Regional T2 and sodium concentration estimates in the normal human brain by sodium-23 MR imaging at 1.5 T J. *Comput Assist Tomogr* 1989, vol 13(4), 561-566.
10. Sharma R, Katz J. Quantitative validation of in vivo intracellular sodium signal acquisition at 4.23 T MRI by applying inversion recovery pulse: First intracellular sodium-cell S phase correlation. ENC conference W &TH P#155, 2001.
11. Kohlar S, Preibisch C, Nittka M, Haase A. Fast three-dimensional sodium imaging of human brain. *MAGMA* 2001, vol 13(2), 63-69.
12. Lin SP, Song SK, Miller JP, Ackerman JJ, Neil JJ. Direct, longitudinal comparison of (1)H and (23)Na MRI after transient focal cerebral ischemia. *Stroke* 2001, vol 32(4), 925-932.
13. Kline R, Wu EX, Petrylak DP, Szabolcs M, Alderson PO, Weisfeldt ML, Cannon PJ, Katz J. Rapid in vivo monitoring of chemotherapeutic response using weighted sodium magnetic resonance imaging. *Clin Cancer Res.* 2000, vol 6(6), 2146-56.
14. Sharma R, Katz J. Minimization of data acquisition in intracellular sodium $[Na]_i$ weighted microimaging using inversion pulse sequence at 4.23 Tesla MRI to correlate increased $[Na]_i$ in apoptosis rich tumors. Proceedings of ISMRM Workshop on "Data Minimization: More Outcome with less" Marco, Florida, 18-21 Oct.2001, pp 68-72.
15. Sharma R, Wu EX, Kline R, Szabolcs M, Cannon PJ, Katz J Rapid in vivo monitoring of methyl-nitroso-urea(MNU) induced breast tumor response to taxotere in rats using intracellular sodium 4.2 Tesla magnetic resonance imaging and immunohistological characterization. Abstract #230 in Proceedings of AACR-NCI-EORTC International Conference at Miami, Florida Oct.27-Nov. 2,2001.

Appendix 1: Inversion Recovery Pulse Sequence source code

```
/****************************************/
Rakesh.PPL
Author: Rakesh Sharma
Date:          August 11, 1999
Version:       1.0 based on Rakesh.ppl
****************************************/
#use RF1 "c:\smis\seqlib\latch31.seq" latch
#use RF1 "c:\smis\seqlib\rfshapes.seq" pf1
#use GRAD "c:\smis\seqlib\gr3040_c.seq" grad
\\ Slice separation is centre to centre NOT slice gap.
/* PARAMLIST
       OBSERVE_FREQUENCY "1H", -20000, 20000, 0, MHz, kHz, Hz, rx1MHz;
       EDITTEXT "Receive Frequency ","Hz ","%i",-32767,32767,0,1,rec_freq;
       SPECTRAL_WIDTH 1000, 400000, 25000, sample_period;
       SCROLLBAR "Phase gradient ","off/on","%u",0,1,1,1,gp_on;
       NO_SAMPLES 64, 512, 256, no_samples;
       DISCARD 0, 10, 0, no_discard;
       SCROLLBAR "Oversample? ","(Yes = 1)","%d",0,1,0,1,oversample;
       NO_VIEWS 1, 512, 48, no_views;
       NO_AVERAGES 1, 30000, 2, no_averages;
       PHASE_CYCLE 1, 4, 2, phase_cycle;
       EDITTEXT "My-phase: 0=off, 2=dc, 4=Cyc","90 deg","%i",0,4,2,1,my_phase;
       EDITTEXT "No. of dummy scan ","1 scan","%i",1,16,4,1,no_dummy;
       EDITTEXT "Patient X angle", "degrees", "%.1f", -1800, 1800, 0, 10, subj_angle_x;
       EDITTEXT "Patient Y angle", "degrees", "%.1f", -900, 900, 0, 10, subj_angle_y;
       EDITTEXT "Patient Z angle", "degrees", "%.1f", -1800, 1800, 0, 10, subj_angle_z;
       GRADIENT_STRENGTH grad_var;
       SLICE_THICKNESS 32767, 1500, gs_var;
       SLICE_SEPARATION -6000, 6000, 1500, slice_offset;
       NO_SLICES 1, 128, 1, no_slices;
```

```
        SLICE_INTERLEAVE 1, 5, 2, slice_interleave;
        FOV 32767,32767,2.0e-3,gr_var,gp_init_var;
        MULTI_ORIENTATION 0, 3, 0, phase_var, r_angle_var, p_angle_var, s_angle_var;
        FOV_SLICE_OFF -12000, 12000, 0, 400, fov_slice_off;
        FOV_PHASE_OFF -32000, 32000, 0, 4000, fov_phase_off;
        FOV_READ_OFF -32000, 32000, 0, 4000, fov_read_off;
        EDITTEXT "Ramp time (multiple of 5 only)","us","%d",100,2000,500,1,tramp;
        EDITTEXT "RF Pulse Shape = ","(1-6)","%d",1,6,6,1,rfnum;
        SCROLLBAR "Obs Mod. power level ","(0 =off)","%u",0,4,1,1,obs_mod_level;
        SCROLLBAR "RF Calibration value ","%","%.2f",0,2047,256,20.48,rfcal;
        SCROLLBAR "Scale for length of hard rf ","%","%d",50,150,100,1,scale_hd;
        SCROLLBAR "Scale for IR 180 rf amplitude ","%","%d",0,200,100,1,scale_ir;
        EDITTEXT "Repetition time","ms","%d",1,2000,300,1,tr;
        EDITTEXT " Inversion time","ms","%d",1,10000,10,1,ti;
        EDITTEXT "Echo time","ms","%d",1,500,30,1,te;
        EDITTEXT "180 FID crusher gradient","us","%d",10,10000,1000,1,tcrush;
        SCROLLBAR "Report Min TE and Tr times? ","(Yes = 1)","%d",0,1,0,1,report_on;
        EDITTEXT "GR: spoil after acq. ","us","%d",0,5000,1000,1,tfilter;
        SCROLLBAR "Read gradient compensation ","DAC UNITS","%d",-500,500,0,1,gr_comp_scale;
        SCROLLBAR "Slice grad. comp. time ","usec","%d",-500,500,0,1,t_gs_comp;
        SCROLLBAR "Slice gradient ","off/on","%u",0,1,1,1,gs_on;
        SCROLLBAR "Read gradient ","off/on","%u",0,1,1,1,gr_on;
        DSP_ROUTINE "c:\smis\dsp";
        DATA_TYPE 0x13;
END */
/* Single/multi-angle oblique switch - do not define this for Single */
#define MAO
#define MAX_SLICE 128
#include "stdfuncs.pph"
#include "stdconvs.pph"
#include "variabl2.pph"
#include "off_mao.pph"
#include "mac3040c.pph"
#include "mac3031c.pph"
void            setsync(int);
long            gp_inc_long;
int             no_rf_lobe,thd180,pIR_mul,my_phase;
int             no_dummy,no_ds;
int             ti_ms,ti_us;
common int      scale_hd, scale_ir,ti;
/*****************************************/
int RS_phase(int nrf, int navg, int ncycle)
{
        int     istep, angle;
        int     p1[6]   = {0,2,0,3,2,1};       \\ first 2 steps for DC_correction
        int     p2[6]   = {0,0,0,0,0,0};       \\ second 4 steps for Cyclops
        int     p3[6]   = {0,2,0,1,2,3};
        istep = navg % ncycle;
        if (ncycle == 4) istep = istep + 2;   \\ Cyclops
        if (nrf == 1)  angle = p1[istep];     \\ rf 90
        if (nrf == 2)  angle = p2[istep];     \\ rf 180
        if (nrf == 3)  angle = p3[istep];     \\ receiver
        return angle;
}
/*****************************************/
main(){
        /* no_discard = 0; */
        view_block = no_averages;
        slice_block = 1;
        asymm = 0;
        #include "testexp.pph"
/* The arguments after each frame name are the pulse length (in usecs) and the pulse width (in Hz)
which are written to the arrays 'rf_length' and 'rf_bwdth' respectively. */
        NEWSHAPE_MAC(1, pf1,"3lobe_sinc_6kHz", 666, 6000)
        NEWSHAPE_MAC(2, pf1,"3lobe_sinc_3kHz", 1332, 3000)
        NEWSHAPE_MAC(3, pf1,"3lobe_sinc_1500Hz", 2664, 1500)
        NEWSHAPE_MAC(4, pf1,"5lobe_sinc_6KHz", 1000, 6000)
        NEWSHAPE_MAC(5, pf1,"5lobe_sinc_3kHz", 2000, 3000)
        NEWSHAPE_MAC(6, pf1,"5lobe_sinc_1500Hz", 4000, 1500)
```

```
/* The phase resolution. */
        phase_increment(1);
        /* discard(no_discard); */
        discard(0);
/* The gradient strengths are negative: gs_var, gr_var and gp_init_var. */
        tacq = sample_period;                \\ long integer
        tacq = (tacq * no_samples)/10L;      \\ acquire time in us.
        tacq_2 = tacq / 2;                   \\ long integer
        tref = tacq_2 - (tramp/2);
        if (rfnum < 4) no_rf_lobe = 3;
        else           no_rf_lobe = 5;
        templ1 = rf_length[rfnum];
        tsel90 = templ1;
        templ2 = templ1 / (no_rf_lobe + 1);
        templ3 = scale_hd * templ2;
        thd180 = templ3 / 50L;
        pulse_bwdth = rf_bwdth[rfnum];
        gr_oversample = oversample + 1;
/* Scale factors defined in the PARAMLIST header (a factor of ten). */
        scale_read_off = 4000;
        scale_slice_off = 400;
        scale_phase_off = 4000;
/* RF deg_90. */
        deg_90 = scale(90,1000, phase_res); /* if phase_res =225 then deg_90 will = 400 */
/* Calculate the phase encode increment(gp_inc). gp_init_var is the initial value passed over from
PARSETUP based on an effective phase encode time of 2 ms. */
        templ1 = gp_init_var;
        templ1 = templ1*2000L;
        templ1 = templ1/(tref + tramp);
        gp_init_var_rescale = templ1;
        gp_inc = scale(templ1, 2,no_views);
        gp_inc_long = scale(templ1, 2,no_views);
        ret = dacmaxlong + templ1;
        if (ret < 0 ){
                printf("FOV too small in phase encode direction");
                goto end;
        }
/* Calculate Gs. */
        templ1 = gs_var;
        templ1 = templ1*pulse_bwdth;
        templ1 = templ1/1500L;
        gs_var_rescale = templ1;
        ret = dacmaxlong + templ1;
        if (ret < 0 ){
                printf(" Slice thickness too small for pulse selected ");
                goto end;
        }
/* GR_COMP is the amplitude of the read preparation pulse. */
        templ3 = gr_var / gr_oversample;
        gr_comp = templ3;
        templ1 = tacq_2 + (tramp/2);
        templ2 = tref + tramp;
        if (templ1 > dacmaxlong ) {
                templ3 = (templ3 * templ1)/ templ2;
        }
        else templ3 = scale( templ3, templ1,templ2);
        ret = dacmaxlong + templ3;
        if (ret < 0 ) {
                printf(" FOV too small for read preparation pulse ");
                goto end;
        }
/* Macro call to avoid initial glitch from 3031 board. */
        MR3031_DEGLITCH
/* Macro call to ouput zeros to 3040 board. */
        BASEMATRIX( subj_angle_z, subj_angle_y, subj_angle_x ) /* Calcluate Base matrix. */
        delay(caldelay,us); /* Matrix calculation delay of 100 us. */
        /* 3040 deglitch call must be made after base matrix call. */
        MR3040_DEGLITCH
```

```
/* 100 usec is the min tramp which sets the clock to 20 ie 20*100ns = 2usec. This is the chosen
minimum setting of the clock. */
        clock = tramp/5;
        MR3040_Clock(clock);
/* Create gradient lists. */
        MR3040_SetListAddress(0);
        slice_list = MR3040_InitList();
        POSPULSE_HOLD()
        read_list = MR3040_InitList();
        POSPULSE_HOLD()
        phase_list = MR3040_InitList();
        POSPULSE_HOLD()
        phase_rec = 0;                /* Reset receiver phase to zero. */
        setsync(2000);                \\ 100 us
        sync();                       /* Synchronise to 100kHz.*/
        starttimer();
        MR3031_setup(latch,"rf_off",0,0,0,0);
        MR3031_go();
        delay(20,us);
/*******MAIN ACQUISITION LOOP ******/
        image_av = 0;
        no_ds = no_dummy;
        dummy_cycles(no_ds);          \\ 1 = dummy, 0 = acquire
averages_loop:
        gp_var=gp_init_var_rescale;   \\ Reset phase encode value for next image.
        current_view = 0;             \\ Counter for P.E. (views) loop.
phase_encode_loop:
        current_view = current_view + 1;
        view_av = 0;                  \\ Counter for view block loop.
view_block_loop:
        current_slice=0;              \\ Counter for multislice loop.
multislice_loop:
        current_slice = current_slice + 1;
        slice_av=0;                   \\ Counter for slice block loop.
        if (no_ds < 1) no_acq = view_av + image_av;
        \\ No. of acquisit. of a given segment of data (used to control phase cycling).
/* Calculate the offsets in terms of frequency and phase increments. */
        SELECTSLICE( current_slice )
        READOFF(fov_read_off, sample_period, scale_read_off,fov_read_freq)
        PHASEOFF(fov_phase_off, phase_res, scale_phase_off, fov_phase_deg)
        SLICEOFF(fov_slice_off, pulse_bwdth, scale_slice_off, fov_slice_freq)
/* RF RECEIVE PHASE INCREMENT TO ACHIEVE OFFSET IN PHASE ENCODE DIRECTION. */
        templ1 = IntToLong(current_view) * IntToLong(fov_phase_deg);
        phase_rec_cal2 = scale(360,1000,phase_res);
        phase_rec = templ1%phase_rec_cal2;
        if (gp_on == 0 ) phase_rec =0; \\ If profile required, then do not change receiver phase.
/* Set up frequency offsets for current slice. */
        frequency_buffer(0);
        frequency(MHz, kHz, Hz, rx1MHz);
        offset_frequency(fov_slice_freq);
/*** Most inner loop **********/
slice_block_loop:
/* RF calibration value. */
        templ1 = rf_length[rfnum];
        tsel90 = templ1;
        templ2 = templ1 / (no_rf_lobe + 1);
        templ3 = scale_hd * templ2;
        thd180 = templ3 / 50L;
        p90_mul = rfcal;
        p180_mul = 2 * rfcal;
        templ1  = p90_mul * scale_IR;
        templ2  = templ1 / 100L;
        pIR_mul = templ2;
/* Calculate delays for accurate echo time. */
        t_refocus = ((tsel90 - tramp)/2) + tcrush + t_gs_comp;
        t_refocus_2 = t_refocus/2;
/* Check that the t_gs_comp selected. */
        if (t_refocus_2 < 4) {
                printf(" t_gs_comp is too negative. \n");
```

```
                goto end;
        }
/* Now calculate make up time to ti and put result in ti_ms, ti_us. */
        templ1  = (thd180/2) + tramp + tsel90 + (tsel90/2);
        templ3  = ti;
        templ3  = (templ3*500L) - templ1;
        ti_ms   = templ3/1000L;
        templ1  = 1000*ti_ms;
        ti_us   = templ3 - templ1;
        if (templ3 < 0 ) {
                US_TO_MS(templ3*2, ret)
                printf(" TI is too short by %d ms\n", - ret);
                goto end;
        }
/* Now calculate make up time to te and put result in te_ms, te_us. */
        templ1  = (tsel90/2) + tcrush + (3*tramp) + tref + (tramp + thd180/2);
        templ3  = te;
        templ3  = (templ3*500L) - templ1;
        te_ms   = templ3/1000L;
        templ1  = 1000*te_ms;
        te_us   = templ3 - templ1;
        if (templ3 < 0 ) {
                US_TO_MS(templ3*2, ret)
                printf(" TE is too short by %d ms\n", - 2*ret);
                goto end;
        }
/* 3 ms to allow for matrix cals and other overhreads in 'tr_min' calculation. Extra 1 ms used in
printf statement to round up to nearest ms value. */
        tr_min = te*1000L + tacq_2 + tfilter + tramp + (tramp + tref + thd180/2) + 3000L;
        tr_min = tr_min + tramp; \\extra delay at pre-90
        tr_extend = ((tr*1000L/no_slices) - tr_min)/1000L;
        if ( tr_extend < 0 ) {
                printf(" TR too short extend by %d ms\n ",
                        (((tr_min-(tr*1000L/no_slices))*no_slices/1000L)+1));
                goto end;
        }
        /* if (report_on == 1) printf(" Min TR = %d ms \n", (tr_min*no_slices/1000L) +1); */
/* Calculations supporting real-time adjustments. Check for overflow. */
        MR3040_SelectMatrix( calc_mat ); /* Select unused matrix during calcs */
        templ3 = gr_comp + gr_comp_scale;
        gr_comp_s = templ3;
        if (templ3 + dacmaxlong < 0) {
                printf("Reduce Read compensation\n");
                goto end;
        }
/* Calculate the matrices for this phase-encode step. Only the phase-encoding and refocus matrices
needs to be rescaled, but recalculate all matrices for real time updates of angulations. */
        CREATE_MATRIX( ss_mat, gs_on*gs_var_rescale, 0,0)
        delay( caldelay, us );
        CREATE_MATRIX(aq_mat, 0, 0, gr_on*gr_var/gr_oversample)
        delay( caldelay, us );
        CREATE_MATRIX(pe_mat, 0, gp_on*gp_var, gr_on*gr_comp_s)
        delay( caldelay, us);
/* Set up receive frequency buffer and select the frequency for the current slice.*/
        frequency_buffer(1);
        frequency(MHz, kHz, Hz, rx1MHz);
        offset_frequency(rec_freq + fov_read_freq);
        frequency_buffer(0);
        reset_frequency();
/* Set phase according to PHASE_CYCLE keyword and acquisition number. */
        ret = 0;
        if (my_phase < 1) {
                phase_90 = aqphase(no_acq,phase_cycle) * deg_90;
                phase_180 = 0;
        }
        else {
                phase_90 = KJ_phase(1,view_av,my_phase) * deg_90;
                phase_180 = KJ_phase(2,view_av,my_phase) * deg_90;
                if (phase_cycle < 2) ret = KJ_phase(3,view_av,my_phase) * deg_90;
```

```
        }
        if (report_on > 0) printf(" RF phases = %d %d \n ", phase_90, ret);
        ret = ret + phase_rec;
        rphase(ret);                          \\ Increment rec phase for offset in pe dirn.
/* Waittimer function used to fix a time of 3ms for overhaed time of create matrix calculations
and loop structures etc. */
        /* if (report_on == 1) printf("te1,te2= %d %d %d %d",te_ms,te_us,te_ms_2,te_us_2); */
        waittimer( 30000 );
        time = hostrequest();
        resync();
/********** SEQUENCE STARTS HERE **********/
        MR3040_SetList( read_list, CHANNEL_R );
        MR3040_SetList( phase_list, CHANNEL_P );
        MR3040_SetList( slice_list, CHANNEL_S );
        MR3040_SelectMatrix( ss_mat );
        MR3040_Clock(clock);                  \\ Extra 3040 clock call for 3040 synchronization.
        phase(0);
        resync();
        if (scale_ir >0) {
                MR3031_HARDPULSE(tramp,thd180,pIR_mul, obs_mod_level);      \\ inversion rf
        }
        else    {
                ret = thd180;
                delay(ret,us);
        }
        if( ti_ms > 0) delay( ti_ms,ms);
        if( ti_us > 4) delay( ti_us,us);
        MR3040_Start(CHANNEL_S);
        starttimer();
        ret = tramp * 10;
        phase(phase_90);
        waittimer(ret);
        ret = tsel90;
        delay(ret,us);
        MR3031_RFSTART(rfnum,pf1,tsel90,p90_mul,tramp, obs_mod_level);      \\ 90 rf
        delay(tcrush,us);
        MR3040_CONTINUE(CHANNEL_S);
        delay(tramp,us);
/* Start phase-encoding and read diphase. */
        MR3040_SelectMatrix( pe_mat );
        MR3040_Start( CHANNEL_R|CHANNEL_P);
        delay(tramp, us);
        delay(tref,us);
        MR3040_Continue( CHANNEL_R|CHANNEL_P);
        starttimer();
        ret = tramp * 10;
        phase(phase_180);
        waittimer(ret);
        MR3040_SelectMatrix( ss_mat );
        MR3040_SetList( slice_list, CHANNEL_S );
        MR3040_SetList( read_list, CHANNEL_R );
        if( te_ms > 0) delay( te_ms,ms);
        if( te_us > 4) delay( te_us,us);
        MR3031_HARDPULSE(tramp,thd180,p90_mul, obs_mod_level);              \\ 180 rf
        /*
        ret = tramp - warmup;
        delay(ret,us);
        ret = thd180 * 10;
        MR3031_setup(latch,"rf_analog_on",0,0,0,p90_mul);
        rfampon(0);
        MR3031_go();
        delay (warmup,us);
        rfpulse(ret, obs_mod_level);
        MR3031_setup(latch,"rf_off",0,0,0,0);
        MR3031_go();
        */
        delay(tramp,us);
        MR3040_Start(CHANNEL_S);
        delay(tramp,us);
```

```
        delay(t_refocus, us);
        MR3040_CONTINUE(CHANNEL_S);
        delay(tramp,us);
        if( te_ms_2 > 0) delay( te_ms_2,ms);
        if( te_us_2 > 4) delay( te_us_2,us);
        starttimer();
        ret = tramp * 10;
        MR3040_SelectMatrix( aq_mat );
        MR3040_Start(CHANNEL_R);
        frequency_buffer(1);
        reset_frequency();
        waittimer(ret);
        resync();
        acquire( sample_period, no_samples );
        delay(tfilter,us);                          \\ GR at post-acquisition
        MR3040_Continue(CHANNEL_R);
        delay(tramp,us);
/* If the time for the execution of hostrequest is > 10 then pause in SCAN has probably been
selected. So, reset 'time' to zero. */
        if (time > 10 ) time = 0;
/* Now calculate the time to make up to the required 'tr-extend'. */
        tr_extend = (tr/no_slices) - tr_min/1000L - time;
        if ( tr_extend > 0 ) delay(tr_extend,ms);
        starttimer();                               \\ time overheads ie matrix calculations etc
        no_acq = no_acq + 1;                        \\ acquisition number (for phase cycling)
        slice_av = slice_av + 1;
        if( slice_av < slice_block )                \\ Slice block
                goto slice_block_loop;
        if (current_slice < no_slices)              \\ Multislicing
                goto multislice_loop;
        if (no_ds > 0) {                            \\ dummy scans
                no_ds = no_ds - 1;
                if (no_ds == 0) dummy_cycles(no_ds); \\ start to acquire
                goto view_block_loop;
        }
        view_av = view_av + slice_block;
        if (view_av < view_block)                   \\ View block
                goto view_block_loop;
        gp_var = gp_init_var_rescale - (current_view * gp_inc_long);
        /* gp_var = gp_var - gp_inc; */
        if (gp_var < -dacmaxlong) {
                printf(" Overflow on GP %d DAC \n ", gp_var);
                goto end;
        }
        if (current_view < no_views)                \\ Phase encode
                goto phase_encode_loop;
        noop;          /* THIS IS NECESSARY AT THE MOMENT AS THEER IS A BUG WITH THE COMPILER */
        image_av = image_av + view_block;
        if (image_av < no_averages)                 \\ Averages
                goto averages_loop;
end:
}
```